

# Fabrication of ZnO nanoparticles in SiO<sub>2</sub> by ion implantation combined with thermal oxidation

H. Amekura,<sup>a)</sup> N. Umeda, Y. Sakuma, and N. Kishimoto

Nanomaterials Laboratory, National Institute for Materials Science (NIMS), 3-13 Sakura, Tsukuba, Ibaraki 305-0003, Japan

Ch. Buchal

Institut fuer Schichten und Grenzflaechen (ISGI-IT), Forschungszentrum Juelich GmbH, D-52425, Juelich, Germany

(Received 14 February 2005; accepted 25 May 2005; published online 29 June 2005)

Zinc-oxide (ZnO) nanoparticles (NPs) are fabricated in silica glasses (SiO<sub>2</sub>) by implantation of Zn<sup>+</sup> ions of 60 keV up to  $1.0 \times 10^{17}$  ions/cm<sup>2</sup> and following thermal oxidation. After the oxidation at 700 °C for 1 h, the absorption in the visible region due to Zn metallic NPs disappears and a new absorption edge due to ZnO appears at  $\sim 3.25$  eV. Cross-sectional transmission electron microscopy confirms the formation of ZnO NPs of 5–10 nm in diameter within the near-surface region of  $\sim 80$  nm thick and larger ZnO NPs on the surface. Under He–Cd laser excitation at  $\lambda = 325$  nm, an exciton luminescence peak centered at 375 nm with FWHM of 113 meV was observed at room temperature. © 2005 American Institute of Physics. [DOI: 10.1063/1.1989442]

Nanometer-size zinc-oxide (ZnO) receives much attention due to the possible applications in high-performance optoelectronic devices.<sup>1,2</sup> In previous experiments we have fabricated metal-oxide nanoparticles (NPs), such as NiO,<sup>3,4</sup> CuO,<sup>5</sup> and Cu<sub>2</sub>O,<sup>6</sup> in silica glasses (SiO<sub>2</sub>) using metal-ion implantation and subsequent thermal oxidation. In this study, this approach is used to form ZnO NPs in SiO<sub>2</sub>. Independently, Chen *et al.*<sup>7</sup> carried out Zn<sup>+</sup> ion implantation into SiO<sub>2</sub> at 160 keV, using fluence up to  $1.0 \times 10^{17}$  ions/cm<sup>2</sup> and a following thermal oxidation step, but they did not obtain clear evidence for the formation of ZnO NPs. Liu *et al.*<sup>8,9</sup> succeeded in the formation of ZnO using a fluence of  $3.0 \times 10^{17}$  ions/cm<sup>2</sup> at the same energy of 160 keV and subsequent thermal oxidation. With increasing the oxidation time, they observed a ZnO signal from the surface by x-ray photoelectron spectroscopy (XPS). They assumed that the ZnO NPs were formed as a layer on the substrate surface, but not in the substrate.<sup>8,9</sup> From their results it is impossible to judge, whether ZnO was formed as NPs or as a thin film. In this study, the depth profile of ZnO NPs has been determined using cross-sectional transmission electron microscopy (XTEM), Rutherford backscattering spectrometry (RBS), and sputtering depth profiling by XPS. Our results show that the ZnO NPs form not only on the surface, but also exist in the SiO<sub>2</sub> substrate.

Optical-grade silica glasses of KU-1 type (OH<sup>−</sup> 820 ppm) of 15 mm diameter and 0.5 mm thickness were implanted with Zn<sup>+</sup> ions of 60 keV up to a fluence of  $1.0 \times 10^{17}$  ions/cm<sup>2</sup>. Since the oxidation processes are governed by diffusional migration of O<sub>2</sub> molecules in the substrate, a lower energy such as 60 keV, i.e., a thinner implanted layer, is better for a homogenous oxidation than higher implantation energy of 160 keV which was used in past studies.<sup>7–9</sup> The ion flux was limited to less than  $2 \mu\text{A}/\text{cm}^2$  in order to maintain a sample temperature below 100 °C during the implantation. The implanted samples were annealed for 1 h in a

tube furnace at a temperature between 400 and 900 °C under flowing O<sub>2</sub> gas.

A dual-beam spectrometer with a resolution of 1 nm was used for the transmittance and reflectance measurements in the wavelength range of 190–1700 nm at room temperature (RT). The absorption was determined from the transmittance and the reflectance, applying corrections for multiple reflections in the sample.<sup>10</sup> Grazing incidence x-ray diffraction (GIXRD) measurements were performed with an incident angle of 3 degrees using a Cr x-ray source to detect the formation of Zn NPs and ZnO NPs. XTEM observation was conducted at an acceleration voltage of 200 kV, to evaluate the size and depth distribution of ZnO NPs. Rutherford backscattering spectrometry (RBS) was carried out to determine the Zn content and the depth profile in as-implanted state and after oxidation, using a 2.06 MeV He<sup>+</sup> beam of 1 mm in diameter with a scattering angle of 160 degrees. Photoluminescence (PL) was excited by the 325 nm line (3.81 eV) from a He–Cd laser. The excitation power and the spot size on the samples were  $\sim 3$  mW and  $\sim 0.4$  mm in diameter, respectively. The spectra were detected by a 30 cm single-monochromator and a CCD array.

Figure 1 shows the absorption spectra of a SiO<sub>2</sub> sample implanted with Zn<sup>+</sup> ions to  $1.0 \times 10^{17}$  ions/cm<sup>2</sup>, in as-implanted state and after oxygen annealing at 600 and 700 °C. In the as-implanted state, a strong and broad peak at  $\sim 4.8$  eV is observed. The peak is ascribed to metallic Zn NPs, because similar peaks were reported in the literature as  $\sim 5$  eV peak in Zn-implanted SiO<sub>2</sub><sup>7</sup> and  $\sim 4.3$  eV peak in Zn-implanted MgO,<sup>11</sup> and both are ascribed to Zn metallic NPs. The formation of Zn metallic NPs in the as-implanted state is confirmed by GIXRD, as shown in Fig. 2. Even in the as-implanted state, the GIXRD spectrum shows relatively sharp peaks which agree well with a powder diffraction spectrum (PDS) of Zn metal,<sup>12</sup> indicating the formation of crystalline Zn NPs. Since the intensity ratios between the diffraction peaks are almost the same as the PDS, no correlated alignment is expected between Zn NPs. As shown in Fig. 1, the absorption spectra show little changes up to 600 °C. After

<sup>a)</sup> Author to whom correspondence should be addressed; electronic mail: amekura.hiroshi@nims.go.jp

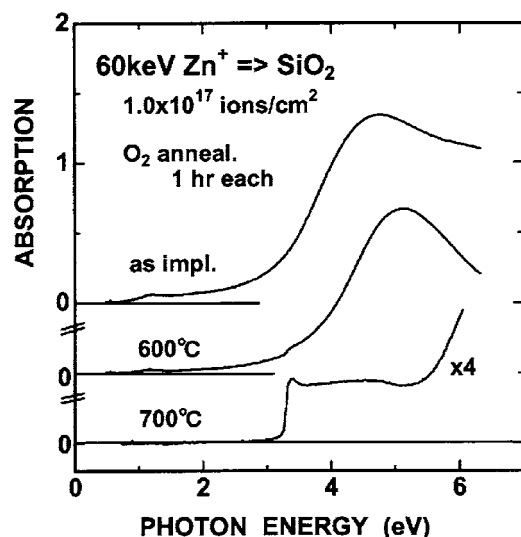


FIG. 1. Absorption spectra of  $\text{SiO}_2$  samples implanted with  $\text{Zn}^+$  ions of 60 keV to  $1.0 \times 10^{17}$  ions/ $\text{cm}^2$ , in as-implanted state, after annealing under oxygen gas flow for 1 h at 600 and 700 °C. The spectra are shifted vertically for clarity. The spectrum after the annealing at 700 °C is four-times magnified ( $\times 4$ ).

annealing at 700 °C for 1 h, drastic changes are induced in the spectra: the absorption in the visible region due to Zn metallic NPs disappears and a new absorption-edge appears around  $\sim 3.25$  eV, with a distinct peak at  $\sim 3.40$  eV. It should be noted that the spectrum after annealing at 700 °C was four times magnified: the absorption decrease in the visible region induced by the oxidation is drastic. The GXR D spectrum shown in Fig. 2 also indicates a drastic transformation from metallic Zn NPs to hexagonal ZnO NPs. Within the detection limit, no diffraction related to Zn metal was observed after oxidation at 700 °C for 1 h. While the diffraction intensity of each line of Zn NPs agrees well with the intensity ratios of the PDS of Zn metal, preferential intensity ratio was observed in ZnO NPs. ZnO (002) diffraction at  $\sim 52$

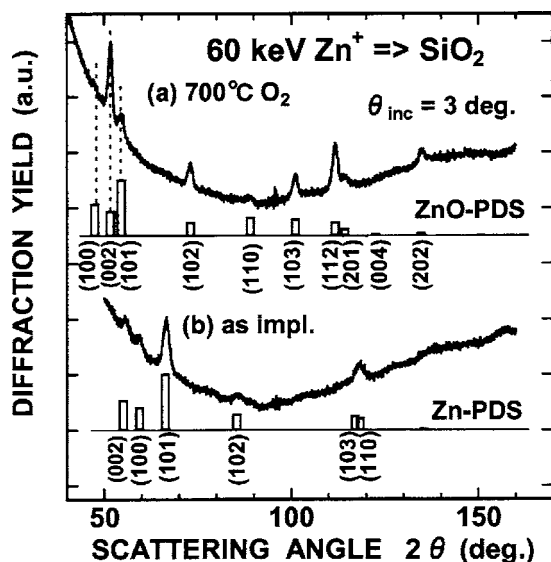


FIG. 2. GXR D patterns of  $\text{SiO}_2$  samples implanted with  $\text{Zn}^+$  ions of 60 keV to  $1.0 \times 10^{17}$  ions/ $\text{cm}^2$ , in as-implanted state and after annealing under oxygen gas flow at 700 °C for 1 h. The incident angle of x-ray was 3°. A Cr x-ray source was used. Powder diffraction patterns of Zn and hexagonal-ZnO from JCPDS library (Ref. 12) are shown as rectangles. The numbers in parentheses indicate the diffraction indices.

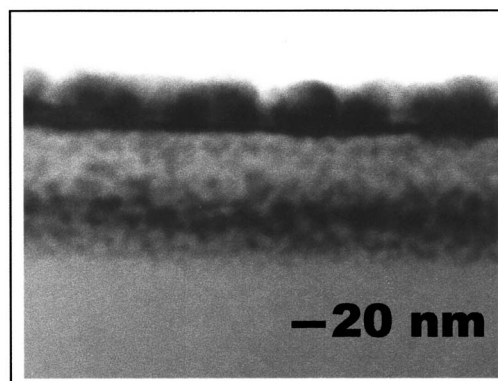


FIG. 3. Cross sectional TEM image of  $\text{SiO}_2$  sample which was implanted with  $\text{Zn}^+$  ions of 60 keV to  $1.0 \times 10^{17}$  ions/ $\text{cm}^2$ , and annealed under oxygen gas flow at 700 °C for 1 h. ZnO NPs are observed as black circles.

degrees is much stronger than ZnO (101) diffraction at  $\sim 55$  degrees in the observed spectrum, while the ZnO (101) diffraction is stronger than ZnO (002) diffraction in the PDS spectrum. ZnO ( $xx2$ ) lines, i.e., ZnO (002), (102), (112), and (202), are more pronounced than other lines.

The XTEM image shown in Fig. 3 clearly confirms that the formation of ZnO NPs not only on the surface but also in the  $\text{SiO}_2$  substrate. NPs of  $\sim 10$  nm in diameter are observed around the projectile range of  $\sim 48$  nm,<sup>13</sup> while smaller NPs of  $\sim 5$  nm in diameter are observed in shallower region. On the surface, droplet-like NPs larger than 30 nm in diameter are observed. As pointed out by Liu *et al.*,<sup>8,9</sup> the NPs on the surface may contribute the preferential orientation of ZnO ( $xx2$ ) direction observed in Fig. 2.

Figure 4 shows the RBS spectra of the sample in the as-implanted state and after thermal oxidation at 700 °C for 1 h. The oxidation at 700 °C for 1 h moves the peak of Zn distribution towards the surface, and extends the other tail of the distribution slightly deeper. The shift of Zn distribution to the surface side is clearly observed in the XTEM image in Fig. 3. This is also confirmed by sputter profiling by XPS and will be reported elsewhere. The Zn content determined

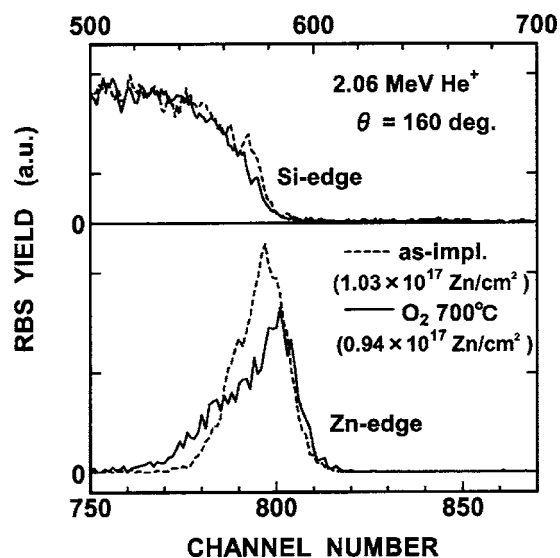


FIG. 4. RBS spectra of  $\text{SiO}_2$  samples implanted with  $\text{Zn}^+$  ions of 60 keV to  $1.0 \times 10^{17}$  ions/ $\text{cm}^2$ , in as-implanted state (broken lines) and after annealing under oxygen gas flow at 700 °C for 1 h (solid lines). The upper half and the lower half show spectra around Si edge and Zn edge, respectively.

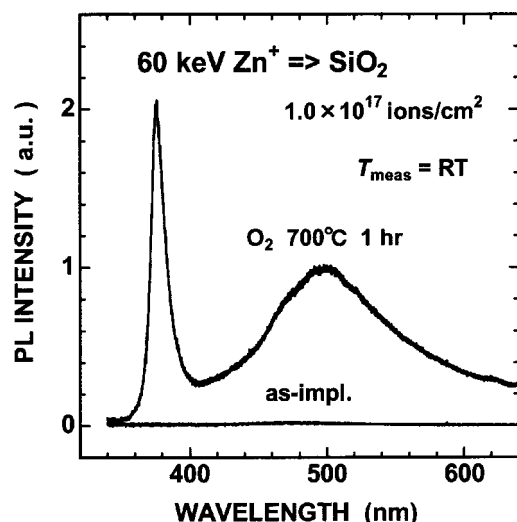


FIG. 5. PL spectra of  $\text{SiO}_2$  samples implanted with  $\text{Zn}^+$  ions of 60 keV to  $1.0 \times 10^{17}$  ions/ $\text{cm}^2$ , in as-implanted state and after annealing under oxygen gas flow at 700 °C for 1 h. PL was excited by a 325 nm line from He–Cd laser of  $\sim 2$  W/ $\text{cm}^2$ .

from the peak area using the RUMP code<sup>14</sup> were  $1.03 \times 10^{17}$  and  $0.94 \times 10^{17}$  ions/ $\text{cm}^2$  in the as-implanted state and after the 700 °C annealing for 1 h, respectively. As shown in Fig. 1, the absorption of the UV region (from  $\sim 3$  to  $\sim 6$  eV) drastically decreases after the oxidation at 700 °C. The decrease of the absorption is mainly due to lower oscillator strength of ZnO NPs in the UV region than Zn NPs, not due to a decrease of the Zn content in the sample.

Under He–Cd laser excitation at 325 nm in wavelength, the sample oxidized at 700 °C for 1 h shows an exciton PL line at 375 nm with FWHM of 113 meV at room temperature, as shown in Fig. 5. The observed FWHM is comparable to literature values of high-purity ZnO grown by plasma-assisted MBE [110 meV (Ref. 15) and 117 meV (Ref. 16)], probably indicating good quality of our ZnO NPs. The sample also shows a broad PL band centered at  $\sim 500$  nm. Since similar PL bands were observed in ZnO thin films<sup>15,16</sup> as deep-level emission, the origin of the PL band around  $\sim 500$  nm in our samples are speculated as the same origin, i.e., deep levels in NPs. In as-implanted state, almost no PL signal was observed. It is contrast with Liu *et al.* who observed a weak but distinct PL peak at  $\sim 380$  nm (Ref. 8)

which could be ascribed to ZnO free-exciton recombination. Liu's results indicate existence of ZnO NPs even in the as-implanted state. This is mysterious because all the Zn ions were implanted within the  $\text{SiO}_2$  and have no chance to interact with an oxygen atmosphere.

In conclusion, we have shown that ZnO NPs are formed in  $\text{SiO}_2$  by ion implantation combined with thermal oxidation at 700 °C for 1 h. ZnO NPs are formed both on the  $\text{SiO}_2$  substrate and in the near-surface layer of  $\sim 80$  nm thick in the substrate. The depth profile of ZnO NPs shifts to the surface side comparing with that of the Zn NPs in the as-implanted state. Relatively strong exciton PL was observed at RT under He–Cd laser excitation.

A part of this study was financially supported by the Budget for Nuclear Research of the MEXT, based on the screening and counseling by the Atomic Energy Commission.

<sup>1</sup>P. Zu, Z. K. Tang, G. K. L. Wong, M. Kawasaki, A. Ohtomo, H. Koinuma, and Y. Segawa, *Solid State Commun.* **103**, 459 (1997).

<sup>2</sup>E. M. Wong and P. C. Searson, *Appl. Phys. Lett.* **74**, 2939 (1999).

<sup>3</sup>H. Amekura, N. Umeda, Y. Takeda, J. Lu, and N. Kishimoto, *Appl. Phys. Lett.* **85**, 1015 (2004).

<sup>4</sup>H. Amekura, N. Umeda, Y. Takeda, J. Lu, K. Kono, and N. Kishimoto, *Nucl. Instrum. Methods Phys. Res. B* (in press).

<sup>5</sup>H. Amekura, Y. Takeda, K. Kono, H. Kitazawa, and N. Kishimoto, *Rev. Adv. Mater. Sci.* **5**, 178 (2003).

<sup>6</sup>H. Amekura, K. Kono, O. A. Plaksin, and N. Kishimoto, *Trans. Mater. Res. Soc. Jpn.* **30** (2005).

<sup>7</sup>J. Chen, R. Mu, A. Ueda, M. H. Wu, Y.-S. Tung, Z. Gu, D. O. Henderson, C. W. White, J. D. Budai, and R. A. Zuhr, *J. Vac. Sci. Technol. A* **16**, 1409 (1998).

<sup>8</sup>Y. X. Liu, Y. C. Liu, D. Z. Shen, G. Z. Zhong, X. W. Fan, X. G. Kong, R. Mu, and D. O. Henderson, *J. Cryst. Growth* **240**, 152 (2002).

<sup>9</sup>Y. X. Liu, Y. C. Liu, D. Z. Shen, G. Z. Zhong, X. W. Fan, X. G. Kong, R. Mu, and D. O. Henderson, *Solid State Commun.* **121**, 531 (2002).

<sup>10</sup>H. Amekura, Y. Takeda, and N. Kishimoto, *Nucl. Instrum. Methods Phys. Res. B* **222**, 96 (2004).

<sup>11</sup>M. A. van Huis, A. van Veen, H. Schut, B. J. Kooi, J. Th. M. De Hosson, X. S. Du, T. Hibma, and R. Fromknecht, *Nucl. Instrum. Methods Phys. Res. B* **216**, 390 (2004).

<sup>12</sup>JCPDS Library, No. 40831 for Zn and No. 361451 for hexagonal-ZnO, International Centre for Diffraction Data.

<sup>13</sup>J. F. Ziegler, J. P. Biersack, and U. Littmark, *The Stopping and Range of Ions in Solids* (Pergamon, New York, 1985), Chap. 8.

<sup>14</sup>L. Doolittle, *Nucl. Instrum. Methods Phys. Res. B* **9**, 344 (1985).

<sup>15</sup>D. M. Bagnall, Y. F. Chen, M. Y. Shen, Z. Zhu, T. Goto, and T. Yao, *J. Cryst. Growth* **184/185**, 605 (1998).

<sup>16</sup>Y. Chen, D. M. Bagnall, H. J. Koh, K. T. Park, K. Hiraga, Z. Zhu, and T. Yao, *J. Appl. Phys.* **84**, 3912 (1998).